# Transcription factors IRF8 and PU.1 are required for follicular B cell development and BCL6-driven germinal center responses

Hongsheng Wang[a,1], Shweta Jain[a], Peng Li[b,c], Jian-Xin Lin[b,c], Jangsuk Oh[b,c], Chenfeng Qi[a], Yuanyuan Gao[a], Jiafang Sun[a], Tomomi Sakai[a], Zohreh Naghashfar[a], Sadia Abbasi[a], Alexander L. Kovalchuk[a], Silvia Bolland[a], Stephen L. Nutt[d,e], Warren J. Leonard[b,c,1], and Herbert C. Morse III[a,1]

[a]Laboratory of Immunogenetics, National Institute of Allergy and Infectious Diseases, National Institutes of Health, Rockville, MD 20852; [b]Laboratory of Molecular Immunology, National Heart, Lung, and Blood Institute, National Institutes of Health, Bethesda, MD 20892; [c]Immunology Center, National Heart, Lung, and Blood Institute, National Institutes of Health, Bethesda, MD 20892; [d]The Walter and Eliza Hall Institute of Medical Research, Parkville, VIC 3052, Australia; and [e]Department of Medical Biology, University of Melbourne, Parkville, VIC 3010, Australia

Contributed by Warren J. Leonard, March 18, 2019 (sent for review January 23, 2019; reviewed by Frederick W. Alt and Jason G. Cyster)

**The IRF and Ets families of transcription factors regulate the expression of a range of genes involved in immune cell development and function. However, the understanding of the molecular mechanisms of each family member has been limited due to their redundancy and broad effects on multiple lineages of cells. Here, we report that double deletion of floxed *Irf8* and *Spi1* (encoding PU.1) by Mb1-Cre (designated DKO mice) in the B cell lineage resulted in severe defects in the development of follicular and germinal center (GC) B cells. Class-switch recombination and antibody affinity maturation were also compromised in DKO mice. RNA-seq (sequencing) and ChIP-seq analyses revealed distinct IRF8 and PU.1 target genes in follicular and activated B cells. DKO B cells had diminished expression of target genes vital for maintaining follicular B cell identity and GC development. Moreover, our findings reveal that expression of B-cell lymphoma protein 6 (BCL6), which is critical for development of germinal center B cells, is dependent on IRF8 and PU.1 in vivo, providing a mechanism for the critical role for IRF8 and PU.1 in the development of GC B cells.**

IRF8 | PU.1 | follicular B cells | BCL6 | germinal center

B cell development in the bone marrow (BM) has been well-characterized as involving three consecutive stages: (*i*) B cell lineage specification and commitment at the pre-pro-B cell stage, (*ii*) pre-B cell receptor (BCR) expression and selection at the pre-B cell stage, and (*iii*) IgM BCR expression and selection at the immature B cell stage. Several transcription factors are vital for progression through these stages. For example, EBF, E2A, and Pax5 are key regulators for B cell lineage commitment and identity maintenance (1). The IFN regulatory factor (IRF) family members IRF4 and IRF8 and Ets family members PU.1 and SpiB are essential for Ig light-chain gene expression and the generation of immature B cells (2–4). Studies of PU.1 null mice demonstrated that PU.1 is a master regulator of the development of all lymphoid and myeloid cells (5). Fine-tuning of PU.1 expression levels determines lymphoid (low concentrations of PU.1) versus myeloid (high concentrations of PU.1) lineage choices (6). By negatively regulating the expression levels of PU.1, IRF8, which is highly expressed in lymphoid progenitors, promotes the development of pre-pro-B cells (4). Understanding how these transcriptional circuits function is important for developing therapeutic strategies to treat hematopoietic diseases.

BM-generated immature B cells migrate to the spleen, where they continue to differentiate into transitional B cells. Studies of several groups have identified subpopulations of transitional (T) B cells that map onto two distinct developmental pathways, namely the T1-premarginal zone (MZ) and T1-T2-T3-follicular (FO) pathways, leading to the eventual emergence of mature MZ and FO B cells, respectively (7). While NOTCH (8–13) and BCR signaling (14–16) have documented roles in determining MZ B cell fate, the transcriptional programs that drive MZ vs. FO B cell lineage selection are largely unknown.

Studies using reporter mice have demonstrated that IRF8 is expressed at high levels in all B cell subpopulations except the plasma cells (PCs) (17). PU.1 is also constitutively expressed in BM-developing B cells and splenic naïve B cells (18). IRF8 binds very weakly on its own to DNA target sequences but is recruited to its binding sites with other transcription factors, such as other IRF family members (IRF1, IRF2, and IRF4) (19–21), Ets family members (PU.1 and TEL) (22, 23), E47, NFATc1, MIZ1 (24–26), AP-1 (27, 28), and BATF (29). Our ChIP-on-ChIP analysis of IRF8 and PU.1 binding sites in lymphomas of germinal center (GC) origin revealed a large number of target sequences, with almost half of them being binding sites for the IRF8–PU.1 heterodimer (30). Given the broad expression patterns and documented functions of IRF8 and PU.1, deletion of either gene in the B lineage might be expected to have profound effects on B cell biology. Surprisingly, however, deletion of either IRF8 or PU.1 alone using

## Significance

**The functions of transcription factors IRF8 and PU.1 in B cell activation and differentiation have been poorly understood due to redundancy between the family members. By using *Mb1*-Cre–mediated B cell-specific deletion of *Irf8* and *Spi1* (encoding PU.1), we provide evidence here that (*i*) double deletion of IRF8 and PU.1 resulted in severe deficiency in follicular and germinal center B cells; (*ii*) antibody affinity maturation was compromised in double-mutant mice; and (*iii*) the expression of BCL6 was dependent on IRF8 and PU.1, indicating the existence of an IRF8/PU.1–BCL6 axis in the initiation phase of the germinal center response. Our data thus reveal that IRF8 and PU.1 are indispensable for the development of late-stage B cells.**

Author contributions: H.W., W.J.L., and H.C.M. designed research; H.W., S.J., P.L., J.-X.L., J.O., C.Q., Y.G., J.S., T.S., Z.N., S.A., and A.L.K. performed research; S.L.N. contributed new reagents/analytic tools; H.W., S.J., P.L., J.-X.L., C.Q., Y.G., J.S., T.S., Z.N., S.A., A.L.K., S.B., S.L.N., and W.J.L. analyzed data; and H.W., P.L., J.-X.L., S.B., S.L.N., W.J.L., and H.C.M. wrote the paper.

Reviewers: F.W.A., Howard Hughes Medical Institute and Boston Children's Hospital, Harvard Medical School; and J.G.C., University of California, San Francisco.

The authors declare no conflict of interest.



Data deposition: The data reported in this paper have been deposited in the Gene Expression Omnibus (GEO) database, https://www.ncbi.nlm.nih.gov/geo (accession no. GSE128166).

[1]To whom correspondence may be addressed. Email: wanghongs@niaid.nih.gov, wjl@helix.nih.gov, or hmorse@niaid.nih.gov.

This article contains supporting information online at www.pnas.org/lookup/suppl/doi:10.1073/pnas.1901258116/-/DCSupplemental.

Published online April 18, 2019.

CD19-Cre–mediated gene excision resulted in only minimal phenotypes (31–33), and immunization with T-dependent antigens resulted in normal antibody responses in these single-mutant mice (31, 32). In the case of PU.1, the minimal phenotype is likely due to redundancy with the closely related family member SpiB, suggesting that at least one of these Ets proteins is required for B cell function (34). In contrast, the importance of the Ets-IRF–binding motifs engaging both IRF8 and PU.1 in B cell function in vivo is not known, and is investigated in this study.

Previous studies using mice bearing an *Irf8* null allele ($Irf8^{-/-}$) and a B cell-specific deletion of PU.1 ($Spi1^{fl/fl}Cd19^{Cre/+}$) revealed a negative regulatory role for IRF8 and PU.1 in PC generation (35), as well as a suppressive function for these factors in the development of pre-B cell acute lymphoblastic leukemia (36). Because $Irf8^{-/-}$ mice exhibited multiple deficiencies in myeloid and lymphoid systems, including excessive generation of myeloid cells and diminished Th1 immune responses (37–39) which may affect the developmental outcome of B cells, we felt it was important to reevaluate the roles of IRF8 and PU.1 in B cell development and function using a B cell-specific gene inactivation system. Because Mb1-Cre mice exhibited earlier expression of the *Cre* gene (at the pro-B stage) than did the CD19-Cre mice (at the pre-B stage) and the former mice also showed higher efficiency in deleting floxed target genes than the latter (40), we used Mb1-Cre–mediated deletion of floxed *Irf8* and *Spi1* loci in B cells in this study. While the previous study by Carotta et al. (35) was carried out mostly in isolated B cells in vitro, we now have focused on analyses of B cell biology in vivo. We found that while early B cell development in the BM was unaffected by deficiency of both IRF8 and PU.1 [termed double-knockout (DKO) mice], these DKO mice had profound defects in FO B cells and GC responses. RNA-seq (sequencing) and chromatin immunoprecipitation (ChIP)-seq analyses revealed IRF8/PU.1–regulated genes that were involved in maintaining the FO B cell phenotype (e.g., *Fcer2a* and *Bach2*) and GC gene programs (e.g., *Bcl6*). Collectively, our results reveal a previously unrecognized role of IRF8/PU.1 in late-stage B cell development.

## Results

**Impaired B Cell Development in DKO Mice.** We generated mice in which both the *Irf8* and *Spi1* genes were inactivated by Mb1-Cre–mediated recombination ($Irf8^{fl/fl}Spi1^{fl/fl}$Mb1-Cre, termed DKO mice). To simplify nomenclature, we herein refer to $Irf8^{fl/fl}Spi1^{fl/fl}$ littermate control mice as $^{+/+}$. As expected, IRF8 and PU.1 proteins were undetectable in splenic B cells isolated from the DKO mice (*SI Appendix*, Fig. S1).

Flow cytometric analyses of early B cell subpopulations in the BM revealed no significant differences in Hardy fractions A through E (41) between DKO and $^{+/+}$ control mice (Fig. 1*A*). However, DKO mice had almost no fraction F (mature recirculating) B cells (Fig. 1*A*). In spleens, the frequencies and total cell numbers of $IgM^{lo/-}IgD^{+}$ FO B cells were significantly reduced, whereas those of MZ B cells ($IgM^{hi}CD21^{+}$) were modestly increased in DKO mice compared with $^{+/+}$ controls (Fig. 1*B*). The numbers of $AA4.1^{+}$ transitional B cells were similar between the two groups (Fig. 1*B*). Immunofluorescence staining of spleen sections revealed normal organization of B cell follicles but with diminished FO and expanded MZ B cell compartments in DKO mice (Fig. 1*C*), consistent with the flow cytometry data (Fig. 1*B*).

Although the frequencies of total B cells in the peritoneum were similar between DKO and $^{+/+}$ mice, the frequencies of B 1a cells were markedly reduced and the B-2/B-1b cells were increased in DKO mice (Fig. 1*D*). It is worth noting that expression of CD23, an identity marker of FO/B-2 cells and a known PU.1 target gene (42), was markedly decreased in splenic and lymph node B cells of DKO mice (*SI Appendix*, Fig. S2*A*), which prevented the use of CD23 as a valid marker for defining transitional and FO B cells in DKO mice. We therefore used staining for IgM, IgD, CD21, and AA4.1 to identify FO B cells. In addition, the expression levels of B220 and CD11b were also down-regulated in B cells (*SI Appendix*, Fig. S2), which limited the use of B220 and CD11b for defining B-1b and B-2 cells in the peritoneum. Nevertheless, the reduction of $IgD^{+}$ B cells in the peritoneum and the fraction F cells in the BM of DKO mice supported a global defect of FO B cell differentiation in DKO mice. Taken together, we conclude that deficiencies in both IRF8 and PU.1 resulted in a profound blockade in FO and B-1a B cell development.

During our analyses, we also examined littermate mice with a genotype of floxed IRF8 only, PU.1 only, or IRF8/PU.1 heterozygous with or without Mb1-Cre (*SI Appendix*, Table S1). While Mb1-Cre–mediated PU.1 deletion alone did not affect B cell distribution in the BM, Mb1-Cre–mediated IRF8 deletion alone appeared to induce a moderate reduction in fraction D, E, and F cells compared with Mb1-Cre controls. This was not observed in $Irf8^{f/f}$*CD19-Cre* mice (31), possibly due to inefficient deletion of *Irf8* by CD19-Cre in early B cells (see later discussion). The lack of significant alterations in early and immature B cells in DKO mice potentially could be due to compensation by transcription factors SpiB and IRF4, which have overlapping functions with PU.1 and IRF8, respectively, in B cell development (34, 36). In addition, the *Mb1-Cre* transgene appeared not to affect B cell numbers in the BM (*SI Appendix*, Table S1), consistent with a previous report (43).

**The FO B Cells in DKO Mice Are Short-Lived.** To determine whether the diminished numbers of FO B cells in DKO mice were due to increased cell death, we employed a standard in vivo BrdU labeling assay to measure the cellular turnover rate over a period of 10 d. As shown in Fig. 2*A*, the numbers of $BrdU^{+}$ FO B cells in DKO mice were significantly higher than in $^{+/+}$ controls throughout the 10-d observation period. In contrast, the BrdU incorporation rates of MZ B cells in DKO mice were essentially equivalent to those of $^{+/+}$ controls. We also examined the apoptosis of ex vivo splenic B cells by detecting caspase activation using a fluorescent irreversible inhibitor of caspases (CaspGLOW) that binds to activated caspase 8. As shown in Fig. 2*B*, DKO B cells including both the MZ/T1 ($CD19^{+}IgM^{+}IgD^{-}$) and FO ($CD19^{+}IgM^{-}IgD^{+}$) subsets exhibited a significant increase in the fraction of cells stained as $CaspGLOW^{+}$. Finally, we performed TUNEL assays to detect apoptotic cells in splenocytes of $^{+/+}$ and DKO mice and found a similar increase in apoptotic cells in DKO compared with controls (Fig. 2*C*). Consistent with the occurrence of enhanced apoptosis in DKO B cells in vivo, we also observed decreased viability in cultured DKO FO B cells compared with $^{+/+}$ controls (Fig. 2*D*). Taken together, these results demonstrated that DKO FO B cells exhibited increased apoptosis and in vivo turnover compared with $^{+/+}$ controls.

**Impaired T-Independent Immune Responses in DKO Mice.** The major changes in the distribution of B cell subpopulations in DKO mice prompted us to examine serum Ig titers (44, 45). Under baseline conditions, DKO mice tended to have higher serum levels of IgM (Fig. 3) and comparable levels of IgA, IgG1, and IgG3 but significantly lower levels of IgG2b and IgG2c compared with $^{+/+}$ controls (Fig. 3*A*). This indicated that class switching to IgG2b and IgG2c was significantly affected by the absence of IRF8/PU.1. Following challenge with a T-independent antigen, NP-Ficoll, both DKO and $^{+/+}$ mice had significantly increased levels of total and NP-specific IgM but only slightly increased levels of total IgM (Fig. 3*B*). Although immunized $^{+/+}$ mice had significantly increased levels of NP-specific IgG3 antibodies, DKO mice had only low levels ($P < 0.05$) (Fig. 3*B*), indicating that IgG3 class switching was also impaired in DKO mice.

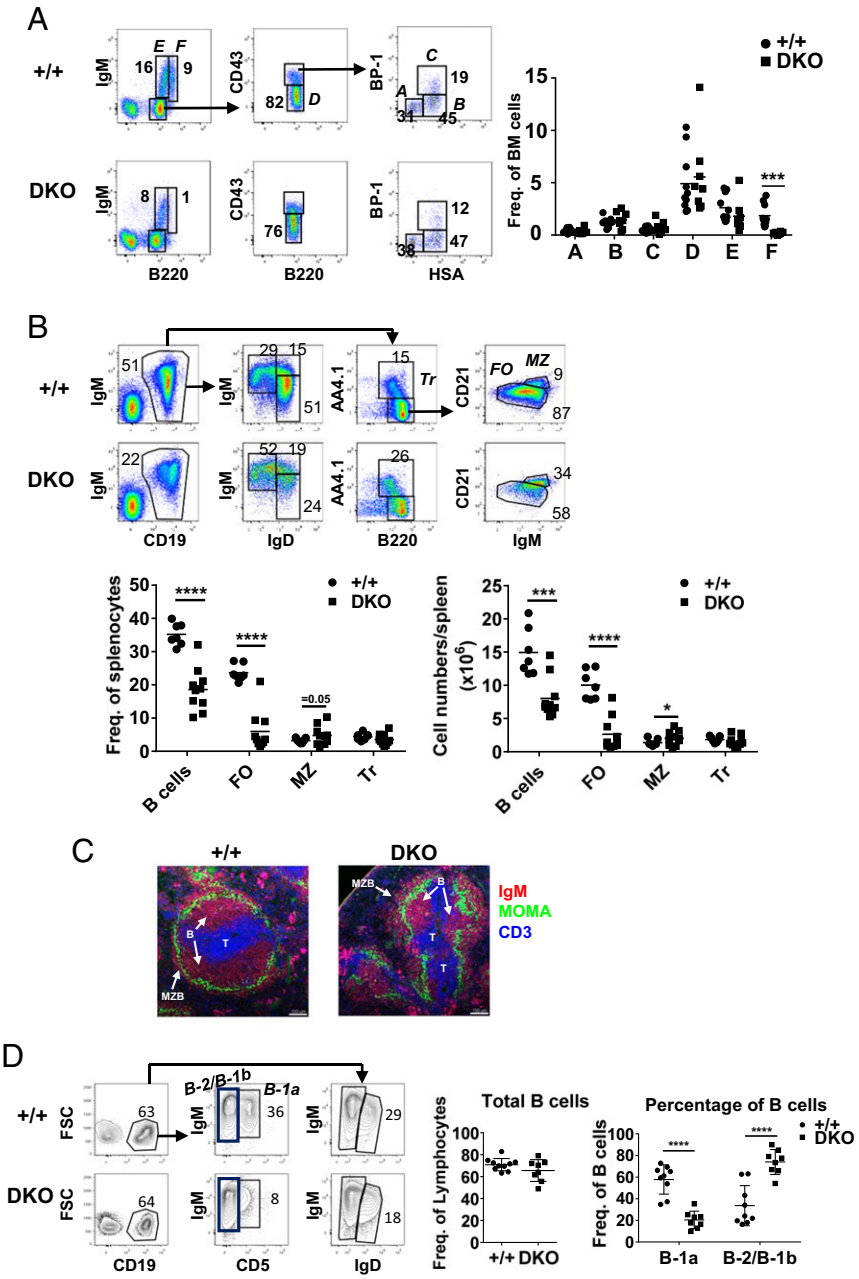


**Fig. 1.** Impact of IRF8/PU.1 loss on B cell subset composition. (*A*, *B*, and *D*) Representative flow cytometry plots of BM (*A*), spleen (*B*), and peritoneum (PerC) (*D*) B cell subsets in DKO and $^{+/+}$ mice. Cells were gated on live lymphocytes. The numbers are percentages of cells falling in each gate. Mean is shown as a horizontal line. Each dot represents a mouse. $*P < 0.05$, $***P < 0.001$, $****P < 0.0001$. (*C*) Representative immunohistochemical staining of spleen sections from the indicated mice. CD3, blue; MOMA, green; IgM, red. (Scale bars, 50 μm.) B, B cell zone [including FO B cells and some shuttling MZ B cells (74)]; MZB, MZ B cells; T, T cell zone.

**Disrupted Germinal Center Responses in DKO Mice.** To determine whether IRF8 and PU.1 are required for T-dependent immune responses, we immunized DKO and control mice with NP-KLH in alum and quantified PC production by enzyme-linked immunospot (ELISpot) assays. Seven days following immunization, the number of NP-specific IgM-secreting PCs was higher in DKO mice than $^{+/+}$ controls (Fig. 4*A*), consistent with a previous report using $Irf8^{-/-}Spi1^{fl/fl}CD19^{Cre/+}$ mice (35). Fourteen days following immunization, the number of $NP^{+}$ IgM-secreting PCs still tended to be higher in DKO mice than $^{+/+}$ controls (Fig. 4*A*). However, the numbers of $NP^{+}$ IgG1-secreting PCs, while not lower in the spleen, were much lower in the BM of DKO mice than $^{+/+}$ controls (Fig. 4*B*). The localization of splenic PCs was found to be in the extrafollicular regions of both mice (*SI Appendix*, Fig. S3). Strikingly, DKO mice did not generate GCs as assessed either by flow cytometry to detect $B220^{+}GL7^{+}FAS^{+}$ GCs in splenocytes of immunized DKO mice (Fig. 4*C*) or by immunohistochemical staining of spleen sections with PNA (Fig. 4*D*). Additionally, mesenteric lymph nodes (MLNs), sites enriched with spontaneous GCs, also had few if any visible $PNA^{+}$ GCs in DKO mice compared with massive dense $PNA^{+}$ GCs in $^{+/+}$ controls (Fig. 4*D*). Taken together, these data demonstrated that the absence of IRF8 and PU.1 enhanced IgM PC development but ablated GC formation.

Consistent with a lack of GCs in DKO mice, generation of antigen-specific class-switched antibodies was also compromised following immunization with NP-KLH. The serum levels of NP-specific IgG1, IgG2b, IgG2c, and IgG3 antibodies were also markedly reduced in DKO mice compared with $^{+/+}$ controls (Fig. 5*A*). The levels of NP-specific IgG1 and IgG2b remained low in DKO mice over the 17-wk period following immunization (Fig. 5*B*).

Generation of high-affinity antibodies is the hallmark of a GC reaction. The lack of GCs in DKO mice prompted us to determine whether IRF8 and PU.1 deficiency would affect production of

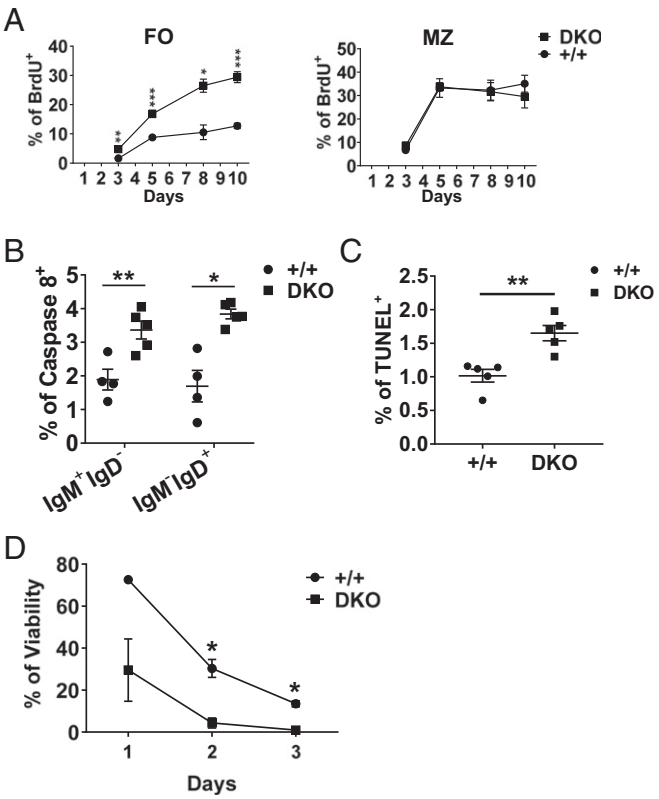


**Fig. 2.** Short half-life of FO B cells in DKO mice. (*A*) Mice were fed with BrdU in drinking water for 10 d. Incorporation of BrdU by FO ($CD19^+IgD^+IgM^-CD21^-$) and MZ ($CD19^+IgD^-IgM^{hi}CD21^+$) B cells was measured by flow cytometry. Two to four (day 3) and three to seven (day 5 to 10) mice were analyzed. Data are mean ± SEM. $*P < 0.05$, $**P < 0.01$, $***P < 0.001$. (*B*) The frequencies of splenic B cells that are caspase $8^+$ among splenic $CD19^+IgM^+IgD^-$ (mostly MZ and T1 and T2) and $CD19^+IgM^-IgD^+$ (mostly FO) cells from the indicated mice are quantified. Each symbol represents one mouse. $*P < 0.05$, $**P < 0.01$. (*C*) Splenocytes were stained with TUNEL reagents and analyzed by flow cytometry. The numbers are frequencies of total splenocytes falling in each gate. Each symbol represents one mouse. $**P < 0.01$. (*D*) Purified splenic B cells were cultured in 10% complete RPMI 1640 medium for the indicated times. Cells were stained with 7AAD and analyzed by flow cytometry. The viable cells were defined as $7AAD^-$. Data are mean ± SE of three mice. $*P < 0.05$.

high-affinity antibodies. We measured serum titers of high-affinity ($NP_4$-reactive) and low-affinity ($NP_{26}$-reactive) antibodies by ELISA. As shown in Fig. 5*C*, the ratios of $NP_4/NP_{26}$ IgM and IgG1 were significantly lower in DKO mice than in $^{+/+}$ controls, indicating that affinity maturation of IgM and IgG1 antibodies was impaired in DKO mice.

Interestingly, the greatly impaired production of class-switched antibodies in immunized DKO mice was in marked contrast to the previous report using *Irf8*$^{-/-}$*Spi1*$^{f/f}$*CD19-Cre* mice that showed increased class switching in vitro (35). To clarify this discrepancy, we stimulated purified B cells from DKO and $^{+/+}$ mice with anti-CD40 plus IL-4 and IL-5. Consistent with previous findings (35), DKO B cells exhibited slightly increased generation of $IgG1^+$ B cells compared with controls. The development of $CD138^+$ PCs was also enhanced in DKO cells (*SI Appendix*, Fig. S4*A*). The proliferation patterns revealed by dilution of the cell tracer CFSE were comparable between DKO and control B cells, but the viability was reduced by 50% in DKO B cells compared with $^{+/+}$ controls. Based on this result, we propose that the lack of class switching in immunized DKO mice is most likely due to an overall low magnitude of GC responses rather than an inability of DKO B cells to undergo class switching. Interestingly, *Aicda* (encoding AID) expression was increased in stimulated DKO B cells in vitro (*SI Appendix*, Fig. S4*B*) (35), consistent with their increased generation of $IgG1^+$ cells (*SI Appendix*, Fig. S4*A*) (35). Our previous studies showed that *Aicda* is a target of IRF8 in human B cells, IRF8 promoting *Aicda* expression in a reporter assay (46). However, our current findings suggest that IRF8 and PU.1 may restrain *Aicda* expression in activated mouse B cells. These data are further complicated by the observation that affinity maturation of NP-specific IgM antibodies, a process requiring AID, was decreased in DKO mice (Fig. 5*C*). How *Aicda* is regulated by IRF8 and PU.1 in vivo remains an open question, as our ChIP-seq analysis revealed only weak PU.1 peaks and no statistically significant IRF8 peaks at the *Aicda* locus (*SI Appendix*, Fig. S5). Nevertheless, our data collectively suggest that IRF8 and PU.1 are required to promote GC formation and antibody affinity maturation.

**IRF8 and PU.1 Regulate Gene Programs for FO and GC B Cell Development.** The marked reduction of FO B cell numbers in DKO mice prompted us to investigate the molecular processes that distinguish DKO and $^{+/+}$ FO B cells. We sort-purified $B220^+AA4.1^-IgM^{lo}IgD^+CD21^-$ FO B cells from spleens and performed transcriptomic analyses using RNA sequencing. By using stringent criteria including differences with a twofold or greater change of expression, expression abundance of at least 5 RPKMs (reads per kilobase of transcript per million mapped reads), and $P$ value < 0.05, we identified 664 genes that were differentially expressed between $^{+/+}$ and DKO FO B cells (146 up-regulated and 518 down-regulated in DKO cells) (Fig. 6*A* and Dataset S1). The most prominent genes down-regulated in DKO FO B cells included the FO B cell identity marker *Fcer2a* (encoding CD23) and *Faim3* (encoding the IgM Fc receptor) (47, 48) and the cell homing and activation markers *Cxcr4*, *Cd83*, *Ly86*, *Ccr6*, *Sell*

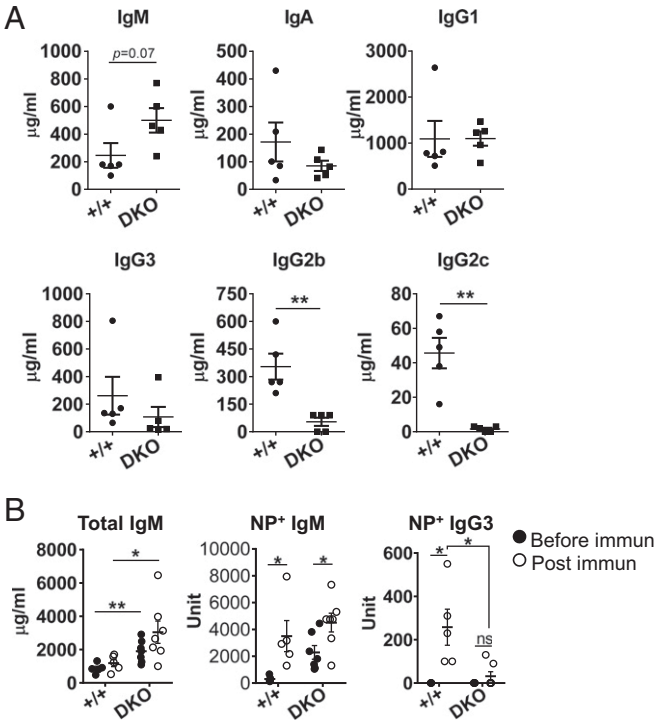


**Fig. 3.** Impaired antibody production in DKO mice. (*A*) Serum Ig levels of naïve DKO and $^{+/+}$ mice were measured by ELISA. (*B*) Mice were immunized with NP-Ficoll and analyzed 7 d later. Antigen-specific antibodies were measured by ELISA. Mean is shown as a horizontal line ±SEM. Each dot represents a mouse. $*P < 0.05$, $**P < 0.01$; ns, not significant.

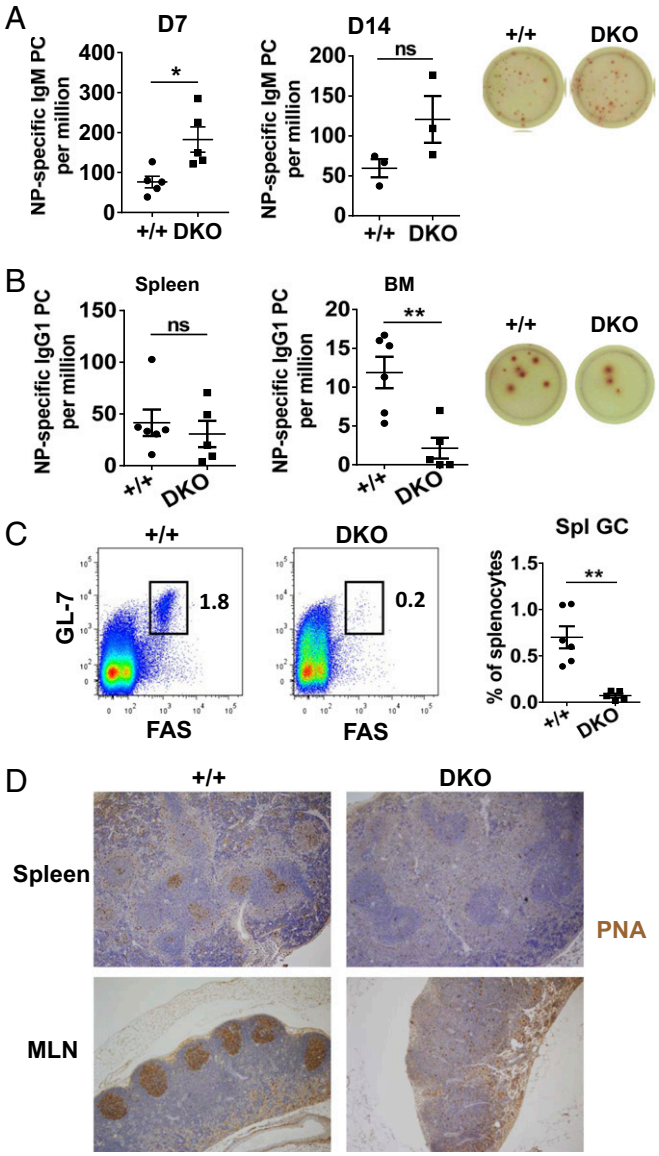


**Fig. 4.** IRF8/PU.1 are essential for GC formation. DKO and $^{+/+}$ mice were immunized i.p. with NP-KLH and alum and analyzed after 7 or 14 d. (*A*) Splenic NP-specific IgM PCs were quantified by ELISpot. (*B*) NP-specific IgM PCs in spleen and BM were quantified by ELISpot. The images represent wells containing typical PCs. (*C*) Splenocytes were stained with anti-B220, GL7, and FAS. Cells were gated on B220$^{+}$ lymphocytes. The numbers are percentages of cells falling in each gate. (*C*, *Right*) A summary of multiple mice. Each dot represents a mouse (*A*–*C*). Mean is shown as a horizontal line ±SEM. Data are representative of four independent experiments. $*P < 0.05$, $**P < 0.01$. (*D*) Immunohistochemical staining for PNA on paraffin-embedded serial sections of spleens and mesenteric lymph nodes. $n = 4$ per group. (Original magnifications, 10×.) Specific staining is shown in brown, and hematoxylin and eosin counterstaining is in blue.

(encoding CD62L), and *Cd40* (Fig. 6*B*). We confirmed differential expression of some of these genes at the protein level by flow cytometry (*SI Appendix*, Fig. S6). In addition, several transcription factors implicated in promoting and maintaining the B cell program, including *Bcl6*, *Mef2c*, *Rel*, and *Bach2*, were significantly decreased in DKO FO B cells (Fig. 6*B*). Interestingly, some of the altered genes, such as *Bcl6*, *Mef2c*, *Fcer2a*, and *Cd83*, were also observed in the previous report using B cells isolated from *Irf8*$^{-/-}$*Spi1*$^{fl/fl}$*Cd19*$^{Cre/+}$ mice (35), with *Bcl6* known to be a direct target of IRF8 (46). Moreover, the mRNA levels of *Tnfrsf13b* (encoding TACI) and *Tnfrsf13c* (encoding BAFF-R), which play pivotal roles in survival of FO B cells (49), were not altered by the absence of IRF8 and PU.1 (*SI Appendix*, Fig. S7), arguing against a possibility that a defective BAFF system may cause the deficiency of FO B cells in DKO mice. However, it remains to be determined whether the BAFF-R signaling pathway was affected by the PU.1/IRF8 mutation and/or whether exogenous BAFF could rescue the FO B cell survival in DKO mice.

Ontology-based functional enrichment analyses of the down-regulated genes led to identification of two sets of genes, affecting either ubiquitin ligase expression or apoptotic processes (Fig. 6*C*). The *Bcl2* family genes *Bcl2*, *Bcl2a1a*, *Bcl2a1b*, and *Bcl2a1d* that are known to be critical for cell survival (50, 51) were significantly down-regulated in DKO B cells (Fig. 6*C*). This is consistent with the increased apoptosis and decreased survival of DKO B cells identified in vivo and in vitro (Fig. 2). Although we did not identify significant numbers of genes that belong to the BCR signaling and PC differentiation pathways, we observed a dramatic enrichment of genes involved in metabolic and cellular processes (Fig. 6*D*). These data suggested that IRF8 and PU.1 control the expression of a large number of genes with broad functions that might be important for the FO B cell program, particularly cell survival.

ChIP-seq analyses using naïve FO B cells identified nearly 8,000 IRF8 binding sites and 23,000 PU.1 binding sites (Fig. 7*A* and Dataset S2). There are several consensus binding sequences for IRF8 and PU.1. The canonical IFN-stimulated response element (ISRE) sequence motif (5′-GAAANNGAAA-3′) contains two IRF binding sites (GAAA). The Ets-binding motif (GGAA)

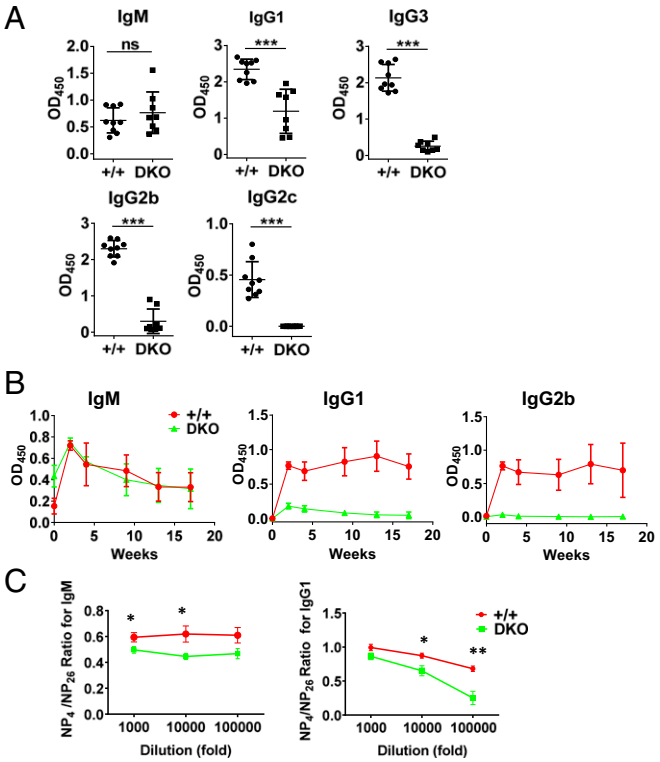


**Fig. 5.** Severely impaired T-dependent antibody responses in DKO mice. (*A* and *B*) Mice were immunized with NP-KLH and alum and analyzed 2 wk (*A*) or up to 17 wk (*B*) later. Serum levels of NP-specific antibodies were measured by ELISA. Each dot represents a mouse. $***P < 0.001$. Error bars represent mean ± SEM of four to six mice per group (*B*). (*C*) Serum NP-specific IgM and IgG1 antibodies were measured by ELISA for high (against $NP_4$-BSA) and low ($NP_{26}$-BSA) affinity binding. Error bars are mean ± SEM of eight or nine mice per group. $*P < 0.05$, $**P < 0.01$.

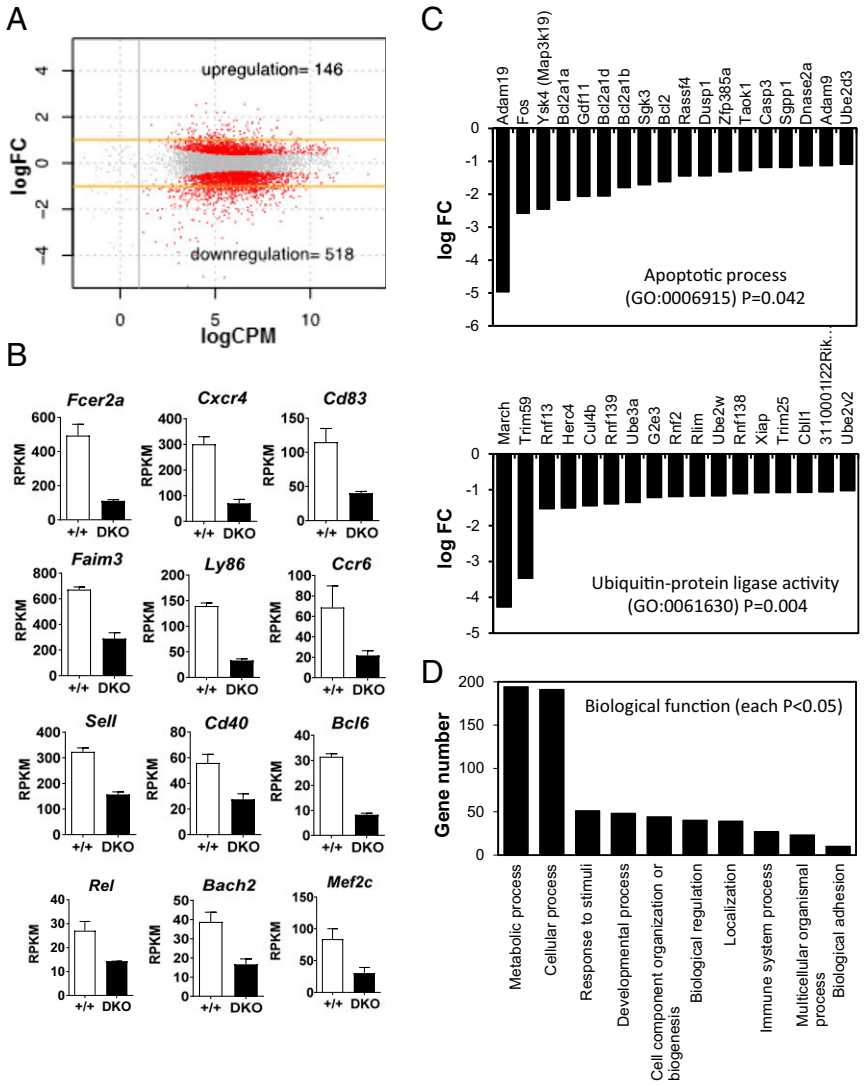


**Fig. 6.** IRF8 and PU.1 regulate FO B cell gene programs. RNA-seq analysis of sort-purified FO B cells ($B220^+AA4.1^-IgM^-IgD^+$) from spleen of DKO and $^{+/+}$ mice. (*A*) Comparisons of genes expressed differentially in $^{+/+}$ versus DKO mice. (*B*) Selected genes that are cell-surface markers critical for FO B cell identity, localization, or transcriptional control. Data are mean RPKM ± SEM for each genotype. (*C*) GO analysis of down-regulated genes in DKO FO B cells. (*C*, *Top*) Differentially regulated genes in the "apoptotic process" (GO:0006915). (*C*, *Bottom*) "Ubiquitin-protein ligase activity" (GO:0061630) gene sets. (*D*) Numbers of genes involved in different biological processes that were enriched in the gene set but down-regulated in the DKO ($P < 0.05$). Analysis in *C* and *D* used the GO-PANTHER slim algorithm.

is found in the Ets-IRF composite element (EICE) [5′-GGAANNGAAA-3′ (22)] and the IRF-Ets composite sequence (IECS) [5′-GAAANN[N]GGAA-3′ (52)]. About 80% of IRF8 binding sites were shared with PU.1, indicating a strong partnership between IRF8 and PU.1 in controlling the FO B cell gene program. Consistent with this view, 43% of differently expressed genes identified by RNA-seq were direct targets of the IRF8–PU.1 heterodimer (Fig. 7*A*). These included *Fcer2a*, *Bcl6*, *Mef2c*, *Ly86*, *Rel*, *Cxcr4*, *Bach2*, and *Cd83*. In previous reports, *Bcl6* and *Mef2c* were shown to be direct targets of IRF8 and PU.1 (35), consistent with our results (Fig. 7*B*). Recently, *Bach2* has been shown to be a target of IRF8 in monocyte dendritic cell progenitors, but the role of PU.1 in this setting is not known (53). *Fcer2a* (CD23) is a known target of PU.1 (42), but previous reports of Carotta et al. and ours did not show if IRF8 can also bind to the *Fcer2a* locus (30, 35). The current identification of these target genes of both IRF8 and PU.1 is important for supporting their biological functions in regulating FO B cell identity, localization, and GC programs. Interestingly, IRF8 preferentially bound to the EICE motif of target genes in naïve FO B cells, whereas IRF8 predominantly occupied the canonical ISRE motif of target genes in activated FO B cells stimulated with anti-IgM plus anti-CD40 for 48 h (Fig. 7*C*). This cell context-dependent binding of IRF8/PU.1 is presumably critical in determining the expression of target genes.

**IRF8 and PU.1 Are Required for BCL6 Expression in Vivo.** We and others previously reported that *Bcl6* is a target of IRF8 and PU.1 based on identification of IRF8-binding sequences in the promoter regions of *Bcl6* and promoter reporter assays (35, 46). The expression levels of the BCL6 transcripts were lower in B cells of DKO mice than in controls (Fig. 6) (35). Because *Bcl6* transcripts are not reliable indicators for protein expression (54, 55), whether IRF8/PU.1 control BCL6 protein levels in vivo is still unknown. We therefore took advantage of DKO mice and measured BCL6 protein levels by intracellular staining and flow cytometric analyses. First, we examined the kinetics of BCL6 expression in purified B cells from DKO and $^{+/+}$ mice stimulated with a mixture consisting of anti-IgM, anti-CD40, IL-4, and IL-21. The expression levels of BCL6 were increased following stimulation and peaked at 2 d in $^{+/+}$ B cells (Fig. 8*A*). In contrast, DKO B cells failed to up-regulate BCL6 expression (Fig. 8*A*). Next, we measured BCL6 protein in ex vivo splenic B cells from immunized mice. Four days following immunization with NP-KLH, DKO mice generated fewer $NP^+$ B cells and the expression level of BCL6 in those $NP^+$ B cells was only half the level in $^{+/+}$ controls (Fig. 8*B*). Seven days after immunization with sheep red blood cells (SRBCs), a strong T-dependent immunogen, DKO mice developed almost no GC B cells and had significantly lower numbers of $IgG1^+$ B cells compared with $^{+/+}$ controls (Fig. 8*C*), paralleling the results obtained above with mice immunized

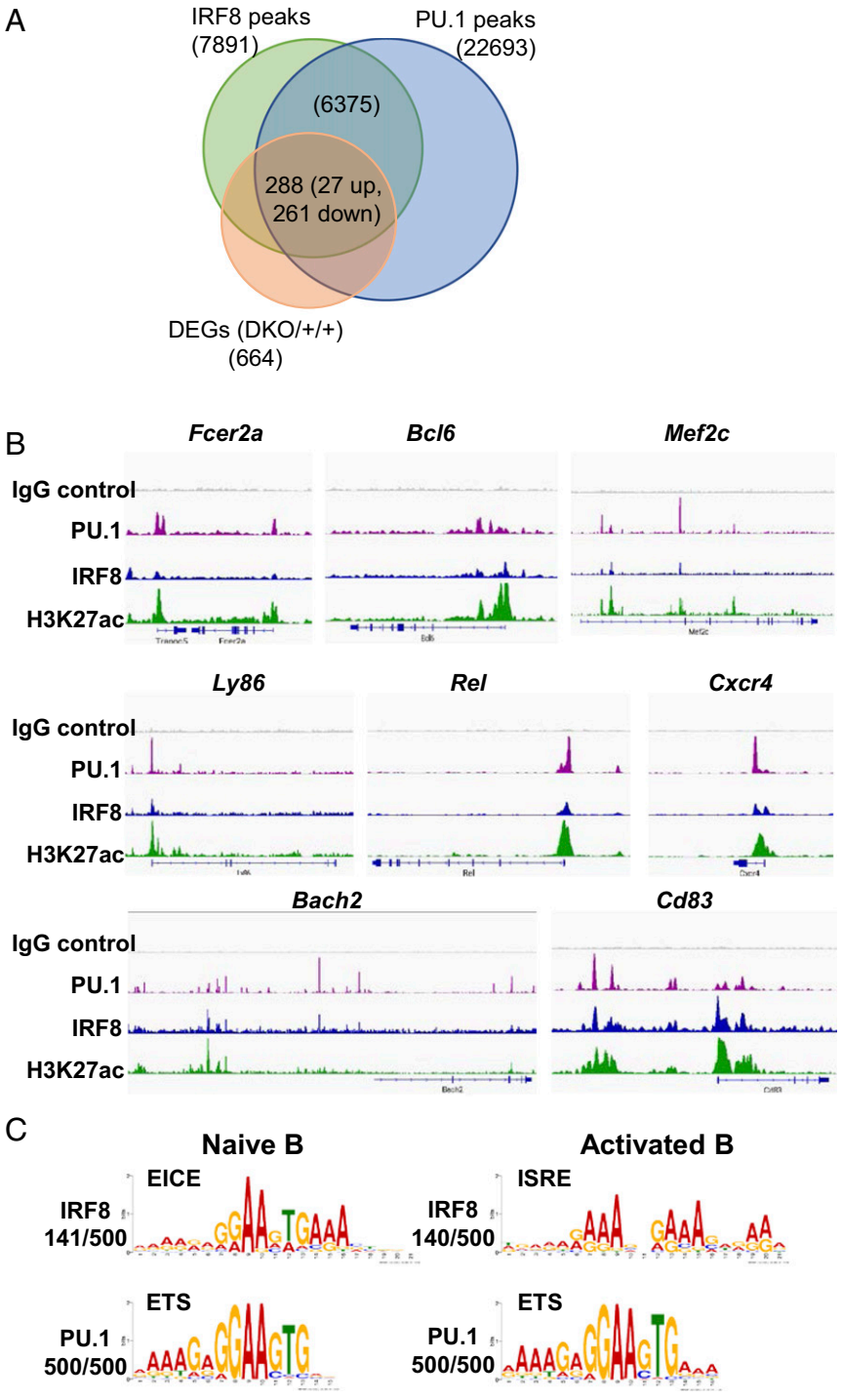


**Fig. 7.** Identification of IRF8/PU.1–binding targets by ChIP-seq analysis. (*A*) Numbers of IRF8 and PU.1 peaks found in naïve FO B cells. DEGs are differently expressed genes by RNA-seq as in Fig. 6. (*B*) Examples of binding patterns in the indicated genes for isotype control IgG and antibodies against PU.1, IRF8, and H3K27ac. (*C*) Motif analyses showing EICE, ETS, and ISRE sequences enriched in naïve vs. activated B cells. Activated B cells were stimulated with anti-IgM plus anti-CD40 for 48 h. The numbers indicate the number of times each motif was counted among the top 500 peaks (sorted by *P* values).

with NP-KLH (Fig. 4 *C* and *D*). In this case, the expression levels of BCL6 protein in $IgG1^+$ B cells were significantly lower in DKO mice than in controls (Fig. 8*D*). As expected, the development of $T_{FH}$ cells and expression levels of BCL6 in $T_{FH}$ cells were comparable between DKO and $^{+/+}$ mice (Fig. 8*E*). Taken together, we conclude that the expression of BCL6 is dependent on IRF8/PU.1 in the early phase of GC formation, which supports a decisive role for IRF8/PU.1 as a regulator of BCL6 expression in GC B cell development.

## Discussion

The results of our study indicate that IRF8 and PU.1 coordinately control the fates of FO and GC B cells through distinct regulatory mechanisms. In FO B cells, IRF8/PU.1 regulate gene expression by binding to the EICE motifs of target genes that maintain FO B cell identity, localization, and survival, whereas in activated B cells the binding landscape of IRF8/PU.1 in target genes shifts to ISRE motifs, which are primarily recognized by IRF8 rather than by both IRF8 and PU.1. This could be due to the fact that in activated B cells, IRF8 expression levels were up-regulated, whereas the expression levels of PU.1 remain unchanged (46, 56). Importantly, we demonstrated that the expression of BCL6, a "master regulator" that regulates the GC transcriptional program, is controlled by IRF8/PU.1 in vivo. In the early phase of a T-dependent immune response, the absence of IRF8/PU.1 failed to up-regulate

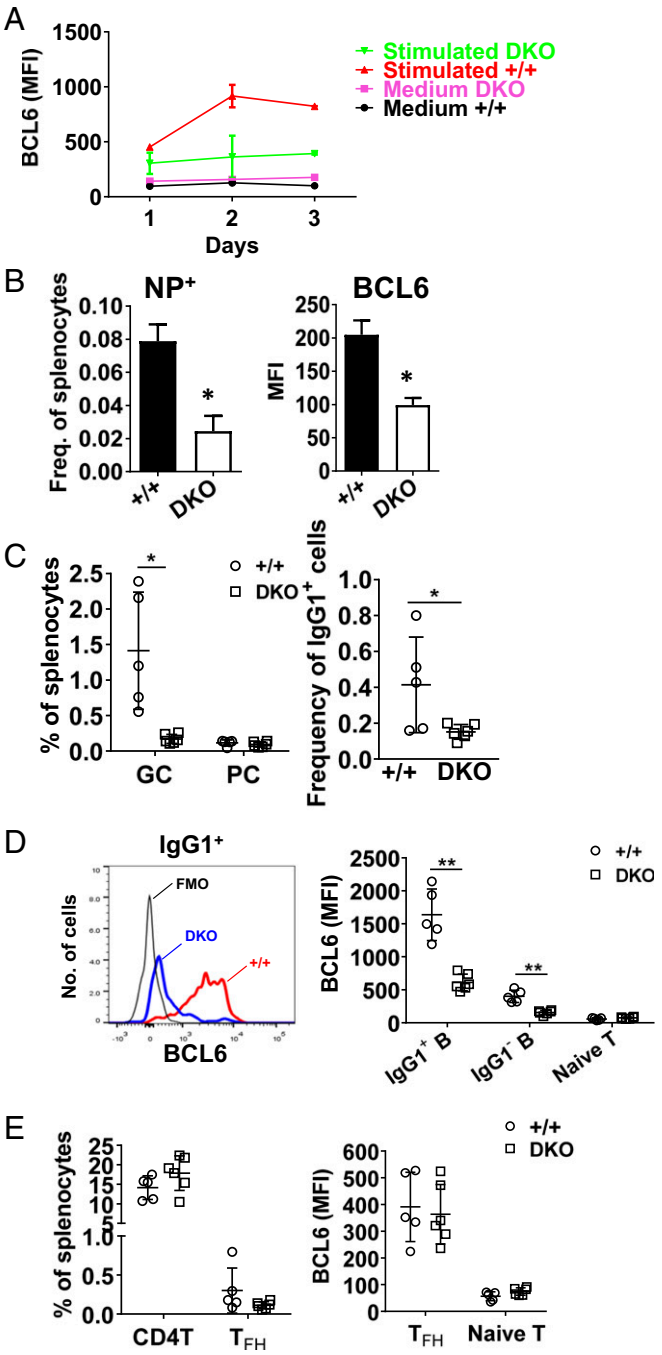


**Fig. 8.** Reduced BCL6 expression in DKO B cells. (*A*) Purified splenic B cells of DKO and $^{+/+}$ mice were stimulated with anti-IgM, anti-CD40, IL-4, and IL-21 for up to 3 d. The cells were fixed, permeabilized, stained with anti-BCL6, and analyzed by flow cytometry. The data represent two independent experiments. Error bars are mean ± SEM of two or three mice per group. (*B*) Mice were immunized with NP-KLH and alum for 4 d. Splenocytes were stained with NP-PE and anti-B220 and BCL6 and analyzed by flow cytometry. Cells were gated on $B220^+$ B cells (*Left*) and $B220^+NP^+$ cells (*Right*). Error bars are mean ± SEM of three or four mice per group. $*P < 0.05$. (*C*) The percentages of GC B cells (gated as in Fig. 4) and PCs ($B220^{lo}CD138^+$) (*Left*) and percentages of $IgG1^+$ B cells (*Right*) of the indicated mice that were immunized with SRBCs for 7 d. (*D*) Intracellular staining of BCL6 in gated $IgG1^+$ B cells. The overlays (*Left*) represent positive staining of BCL6, and the dot plots (*Right*) are the mean fluorescence intensity (MFI) of BCL6 of multiple mice. Each dot represents a mouse. (*E*) The frequency of T cell subsets in SRBC-immunized mice (*Left*) and MFI of BCL6 in T cells of DKO and $^{+/+}$ mice. $T_{FH}$ cells were gated as $CD4^+PD\text{-}1^+CXCR5^+ICOS^+$ (75). Each dot represents a mouse. Mean is shown as a horizontal line ±SD. $*P < 0.05$, $**P < 0.01$.

BCL6 proteins, which correlates with a complete lack of GC formation and high-affinity antibody production. These results establish a paradigm that IRF8/PU.1 functions upstream of BCL6 and mechanistically works as an initiator for GC development.

In a previous report using $Irf8^{-/-}Spi1^{fl/fl}Cd19^{Cre/+}$ and $Irf8^{fl/fl}Spi1^{fl/fl}Cd19^{Cre/+}$ mice, the reduction in FO B cell numbers was moderate compared with our $Irf8^{fl/fl}Spi1^{fl/fl}Mb1^{Cre/+}$ DKO mice. This could be due to incomplete CD19-Cre activity in early B cells (57). It was shown that the deletion efficiency of CD19-Cre is 33 to 75% in BM B cells and 80 to 90% in splenic B cells (40). However, the Mb1-Cre used in this study achieves a deletion efficiency of >95% in both BM and spleen B cells (40). It is also worth noting that $Irf8^{-/-}$ mice have a broad array of defects in their myeloid and lymphoid systems. These include excessive generation of myeloid cells, which results in hypercellular BM and splenomegaly with disrupted follicular architecture (37, 38, 46). Moreover, the development of plasmacytoid dendritic cells and Th1 cells is also impaired in $Irf8^{-/-}$ mice (39, 58, 59). This abnormal microenvironment in the $Irf8^{-/-}$ background may alter normal B cell development.

Previous studies using RNA-seq and $Irf8^{-/-}Spi1^{fl/fl}Cd19^{Cre/+}$ (35) or PU.1/SpiB DKO (34) mice revealed a range of IRF8/PU.1–regulated genes in B cells but did not provide direct evidence of co-occupancy of most of those genes by IRF8 and PU.1. We previously analyzed mouse B cell lymphomas with a GC origin using ChIP-on-ChIP technology and identified ∼140 genes that were direct targets of IRF8–PU.1 dimers (30). In the current study, we employed ChIP-seq technology and integrated these data with RNA-seq analyses of naïve and activated FO B cells to reveal a large number of novel targets of IRF8 and PU.1. These include *Fcer2a* (CD23), an FO B cell identity marker, *Cxcr4*, important for FO B cell positioning, as well as *Bach2* (60) and *Cd83* (61), which are known to play a role in B cell differentiation and activation (Fig. 7*B*). Careful comparison of $Bach2^{-/-}$ mice with DKO mice revealed similar phenotypes: Both strains exhibited significantly reduced FO B cell numbers, severely impaired class-switch recombination, and the absence of GCs (60). Interestingly, the promoter regions of *Bach2* have multiple binding peaks for IRF8 and PU.1 (Fig. 7*B*), indicating that *Bach2* is a target of both IRF8 and PU.1 in B cells. It will be interesting in the future to determine if BACH2 is a mediator of the actions of IRF8/PU.1, and if overexpression of BACH2 can restore FO B cell development in IRF8/PU.1 DKO mice.

GC development includes phases of initiation and expansion guided by a coordinated transcriptional network that is thought to involve at least 15 transcription factors (reviewed in ref. 62). Among the best studied, BCL6 is central to GC differentiation, and $Bcl6^{-/-}$ mice do not form GCs (63–65). BCL6 represses the PC program by suppressing the *Prdm1* locus (66, 67), which enables GC B cells to instead undergo multiple rounds of expansion and antigen selection. Repression of *Bcl6* by IRF4 and Blimp1 is required for GC differentiation into PCs (68, 69). Competition between IRF8 and IRF4 in binding to common target genes including BCL6 has been proposed as a mechanism for fate control of GCs and PCs (33, 35). Following immunization with a protein antigen, IRF4 is transiently induced during GC formation, and high concentrations of IRF4 antagonize the GC fate (70). In contrast, PU.1 and SpiB act redundantly to control the GC response (34). These results are consistent with the idea that during the early phase of GC development, IRF4 and IRF8 together with PU.1 or SpiB may have synergistic effects on BCL6 induction, whereas the gain of IRF4 activity and the down-regulation of PU.1 and SpiB in late-stage GCs are essential for PC development. Our data showed that following stimulation, as early as day 1 in vitro and day 4 in vivo, the expression level of BCL6 proteins was up-regulated in B cells of normal mice. However, IRF8/PU.1 deficiency failed to stimulate BCL6 expression. In conjunction with our previous findings that

IRF8 expression is rapidly up-regulated in stimulated IRF8-EGFP reporter B cells that were stimulated with anti-BCR antibody, LPS, or anti-CD40 plus IL-4 (17), these data position IRF8/PU.1 upstream of BCL6 during the initiation phase of GC formation. We propose a model that in the beginning of a GC response, activated B cells increase IRF8 expression, which together with PU.1 stimulates BCL6 protein production, which then regulates downstream GC gene programs.

In summary, our data demonstrate that IRF8 and PU.1 double deficiency in B cells impairs the development of FO and GC B cells. Our ChIP-seq analyses have revealed distinct regulatory mechanisms by IRF8 and PU.1 in regulating FO and GC B cell fates by binding to different consensus sequences of target genes in a cell context-dependent manner. The identification of an IRF8/PU.1–BCL6 axis sheds light on our understanding of how early GC B cells are regulated by this transcriptional network. Further understanding of the molecular mechanisms by which IRF8 and PU.1 regulate late stages of B cell differentiation may lead to new strategies for enhancing beneficial high-affinity antibody responses and repressing pathogenic antibody responses.

## Materials and Methods

**Mice.** B6, *Irf8*$^{f/f}$, and *Spi1*$^{f/f}$ mice were described previously (31, 32). *Mb1*-Cre mice (40) were purchased from the Jackson Laboratory. All mice were maintained in a specific pathogen-free facility at the National Institutes of Health according to guidelines approved by National Institute of Allergy and Infectious Diseases (ASP LIG-16) Animal Care and Use Committees. Littermate control mice were used throughout the study.

**Flow Cytometry.** Cells were prepared and stained as previously reported (71). Resources of antibodies specific for cell-surface markers and intracellular proteins are listed in *SI Appendix*, Table S2. Stained cells were analyzed using an LSR II analyzer (BD Biosciences) and FlowJo software. Dead cells were excluded by gating on cells negative for a viability dye (7AAD, propidium iodide, or fixable viability dye eFluor506). Doublets were excluded electronically by setting an SSC-A vs. FCS-W gate. For some experiments, cells were sorted by a FACSAria sorter (BD Biosciences).

For in vitro stimulation, cells were cultured in complete RPMI 1640 medium supplemented with 10% FBS in the presence (or not) of anti-IgM [F(ab′)$_2$] (10 μg/mL), CD40 (2 μg/mL), IL-4 (10 ng/mL), and IL-21 (20 ng/mL) for up to 3 d.

**BrdU Labeling, CaspGLOW, and TUNEL Assays.** Mice were given drinking water supplemented with 0.5 mg/mL 5-bromo-2′-deoxyuridine (BrdU; Sigma-Aldrich) and 1 mg/mL dextrose continuously for 10 d using a protocol of BrdU Flow Kits (BD Pharmingen). At different time points, mice were killed and spleens were analyzed by flow cytometry according to the supplier's instructions.

For the CaspGLOW assay, splenic cells were stained with a CaspGLOW Fluorescein Active Caspase-8 Staining Kit (Thermo Fisher Scientific) according to the manufacturer's instructions. The cells were then stained with antibodies against CD19, IgM, and IgD and analyzed by flow cytometry. For the TUNEL assay, splenocytes were treated with ethanol and reagents supplied by the APO-BrdU TUNEL Assay Kit (Invitrogen), followed by flow cytometry.

**Immunization and Antibody Detection.** For T-independent immune responses, mice were immunized i.p. with 20 μg of NP-Ficoll (Biosearch). Blood samples were taken before and 7 d after immunization. For T-dependent immune responses, mice were immunized i.p. with 100 μg of NP-KLH (Biosearch) in alum or 0.5 mL of sheep red blood cells (10% diluted with PBS). Blood samples were taken every 2 wk after immunization.

Serum antibodies were tested by ELISA. For antigen nonspecific total antibodies, 96-well plates were coated with polyclonal anti-IgM or other isotype-specific antibodies. For antigen-specific antibodies, the plates were coated with NP(23)-BSA or NP(4)-BSA (Biosearch). After blocking with 1% BSA, diluted serum samples were incubated for 2 h, followed by incubation with secondary HRP-conjugated mouse-specific anti-Ig isotype antibodies and substrate OPD (Sigma-Aldrich). The reaction was read at 450 nm using a SpectraMax Plus 384 microplate reader (Molecular Devices).

**ELISpot Assay.** Spleen and BM PCs were quantified by NP-specific Ig ELISpot assays. Briefly, aliquots of 1.25 to 5.0 × 10$^5$ spleen and BM cells were plated in triplicate in NP-BSA–precoated 96-well PVDF membrane plates (Millipore) and incubated overnight at 37 °C in 5% $CO_2$. The plates were washed with PBS containing 0.05% Tween 20 and incubated with HRP-conjugated anti-mouse IgM or IgG1 (Jackson ImmunoResearch Laboratories), followed by reaction with FAST 5-bromo-4-chloro-3-indolyl phosphate/NBT chromogen substrate (Sigma-Aldrich). The plates were scanned with a CTL ImmunoSpot S5 Core Analyzer (Cellular Technology) and analyzed by ImmunoSpot software 4.0 (Cellular Technology).

**RNA-Seq and ChIP-Seq.** FACS-purified FO B cell subsets were extracted for RNA by using an RNeasy Mini Kit (Qiagen) including a DNA digestion step according to the manufacturer's instructions. RNA-seq analyses were performed as described previously (72). Gene ontology (GO) analysis was carried out with the PANTHER GO-slim classification tool of the GO Reference Genome Project (ref. PMID 26578592).

ChIP-seq was performed as previously reported (72, 73) using antibodies against IRF8 (clone D20D8; Cell Signaling Technology), acetyl-histone H3 (Lys27) (D5E4, Cell Signaling Technology), and PU.1 (sc-390405 X; Santa Cruz). Ex vivo FO B cells were prepared by sorting and processed for fixation and ChIP. For activated B cells, sort-purified FO B cells were cultured in complete RPMI 1640 medium in the presence of F(ab′)$_2$ anti-IgM (10 μg/mL) plus anti-CD40 (2 μg/mL) and IL-4 (10 ng/mL) for 2 d. The cells were then processed for ChIP.

**Immunohistochemistry and Immunofluorescence Staining.** Paraffin sections of spleen and MLN tissues were processed and stained with PNA or anti-CD138 Ab by the Pathology/Histotechnology Laboratory of the National Cancer Institute. Slides were imaged with an Olympus BX41 microscope (10× and 40× objectives) equipped with an Olympus DP71 camera. In other cases, cryopreserved splenic sections were stained with antibodies against IgM, CD3, and MOMA and imaged using a Nikon ECLIPSE TE2000-U confocal microscope.

**Statistical Analysis.** Two-tailed Student's *t* test was used to determine the statistical significance of the data. $P < 0.05$ was considered to be statistically significant.

**ACKNOWLEDGMENTS.** We thank Alfonso Macias and Bethany Scott for managing the mouse colony. This work was supported in part by the Intramural Research Program of the NIH, NIAID (H.W., S.J., C.Q., Y.G., J.S., T.S., Z.N., S.A., A.L.K., S.B., and H.C.M.), and NHLBI (P.L., J.-X.L., J.O., and W.J.L.). S.L.N. was supported by grants from the National Health and Medical Research Council of Australia (1054925, 1058238).

1. Fuxa M, Skok JA (2007) Transcriptional regulation in early B cell development. *Curr Opin Immunol* 19:129–136.
2. Batista CR, Li SK, Xu LS, Solomon LA, DeKoter RP (2017) PU.1 regulates Ig light chain transcription and rearrangement in pre-B cells during B cell development. *J Immunol* 198:1565–1574.
3. Lu R, Medina KL, Lancki DW, Singh H (2003) IRF-4,8 orchestrate the pre-B-to-B transition in lymphocyte development. *Genes Dev* 17:1703–1708.
4. Wang H, et al. (2008) IRF8 regulates B-cell lineage specification, commitment, and differentiation. *Blood* 112:4028–4038.
5. Scott EW, Simon MC, Anastasi J, Singh H (1994) Requirement of transcription factor PU.1 in the development of multiple hematopoietic lineages. *Science* 265:1573–1577.
6. DeKoter RP, Singh H (2000) Regulation of B lymphocyte and macrophage development by graded expression of PU.1. *Science* 288:1439–1441.
7. Allman D, Pillai S (2008) Peripheral B cell subsets. *Curr Opin Immunol* 20:149–157.
8. Hozumi K, et al. (2004) Delta-like 1 is necessary for the generation of marginal zone B cells but not T cells in vivo. *Nat Immunol* 5:638–644.
9. Kuroda K, et al. (2003) Regulation of marginal zone B cell development by MINT, a suppressor of Notch/RBP-J signaling pathway. *Immunity* 18:301–312.
10. Moran ST, et al. (2007) Synergism between NF-kappa B1/p50 and Notch2 during the development of marginal zone B lymphocytes. *J Immunol* 179:195–200.
11. Saito T, et al. (2003) Notch2 is preferentially expressed in mature B cells and indispensable for marginal zone B lineage development. *Immunity* 18:675–685.
12. Tanigaki K, et al. (2002) Notch-RBP-J signaling is involved in cell fate determination of marginal zone B cells. *Nat Immunol* 3:443–450.
13. Witt CM, Won WJ, Hurez V, Klug CA (2003) Notch2 haploinsufficiency results in diminished B1 B cells and a severe reduction in marginal zone B cells. *J Immunol* 171:2783–2788.
14. Carey JB, Moffatt-Blue CS, Watson LC, Gavin AL, Feeney AJ (2008) Repertoire-based selection into the marginal zone compartment during B cell development. *J Exp Med* 205:2043–2052.
15. Martin F, Kearney JF (2000) Positive selection from newly formed to marginal zone B cells depends on the rate of clonal production, CD19, and btk. *Immunity* 12:39–49.
16. Wen L, et al. (2005) Evidence of marginal-zone B cell-positive selection in spleen. *Immunity* 23:297–308.
17. Wang H, et al. (2014) A reporter mouse reveals lineage-specific and heterogeneous expression of IRF8 during lymphoid and myeloid cell differentiation. *J Immunol* 193:1766–1777.

18. Nutt SL, Metcalf D, D'Amico A, Polli M, Wu L (2005) Dynamic regulation of PU.1 expression in multipotent hematopoietic progenitors. *J Exp Med* 201:221–231.
19. Bovolenta C, et al. (1994) Molecular interactions between interferon consensus sequence binding protein and members of the interferon regulatory factor family. *Proc Natl Acad Sci USA* 91:5046–5050.
20. Rosenbauer F, et al. (1999) Interferon consensus sequence binding protein and interferon regulatory factor-4/Pip form a complex that represses the expression of the interferon-stimulated gene-15 in macrophages. *Blood* 94:4274–4281.
21. Sharf R, et al. (1995) Functional domain analysis of interferon consensus sequence binding protein (ICSBP) and its association with interferon regulatory factors. *J Biol Chem* 270:13063–13069.
22. Brass AL, Kehrli E, Eisenbeis CF, Storb U, Singh H (1996) Pip, a lymphoid-restricted IRF, contains a regulatory domain that is important for autoinhibition and ternary complex formation with the Ets factor PU.1. *Genes Dev* 10:2335–2347.
23. Kuwata T, et al. (2002) Gamma interferon triggers interaction between ICSBP (IRF-8) and TEL, recruiting the histone deacetylase HDAC3 to the interferon-responsive element. *Mol Cell Biol* 22:7439–7448.
24. Alter-Koltunoff M, et al. (2003) Nramp1-mediated innate resistance to intraphagosomal pathogens is regulated by IRF-8, PU.1, and Miz-1. *J Biol Chem* 278: 44025–44032.
25. Nagulapalli S, Atchison ML (1998) Transcription factor Pip can enhance DNA binding by E47, leading to transcriptional synergy involving multiple protein domains. *Mol Cell Biol* 18:4639–4650.
26. Zhu C, et al. (2003) Activation of the murine interleukin-12 p40 promoter by functional interactions between NFAT and ICSBP. *J Biol Chem* 278:39372–39382.
27. Glasmacher E, et al. (2012) A genomic regulatory element that directs assembly and function of immune-specific AP-1-IRF complexes. *Science* 338:975–980.
28. Li P, et al. (2012) BATF-JUN is critical for IRF4-mediated transcription in T cells. *Nature* 490:543–546.
29. Tussiwand R, et al. (2012) Compensatory dendritic cell development mediated by BATF-IRF interactions. *Nature* 490:502–507.
30. Shin DM, Lee CH, Morse HC, III (2011) IRF8 governs expression of genes involved in innate and adaptive immunity in human and mouse germinal center B cells. *PLoS One* 6:e27384.
31. Feng J, et al. (2011) IFN regulatory factor 8 restricts the size of the marginal zone and follicular B cell pools. *J Immunol* 186:1458–1466.
32. Polli M, et al. (2005) The development of functional B lymphocytes in conditional PU.1 knock-out mice. *Blood* 106:2083–2090.
33. Xu H, et al. (2015) Regulation of bifurcating B cell trajectories by mutual antagonism between transcription factors IRF4 and IRF8. *Nat Immunol* 16:1274–1281.
34. Willis SN, et al. (2017) Environmental sensing by mature B cells is controlled by the transcription factors PU.1 and SpiB. *Nat Commun* 8:1426.
35. Carotta S, et al. (2014) The transcription factors IRF8 and PU.1 negatively regulate plasma cell differentiation. *J Exp Med* 211:2169–2181.
36. Pang SH, et al. (2016) PU.1 cooperates with IRF4 and IRF8 to suppress pre-B-cell leukemia. *Leukemia* 30:1375–1387.
37. Wang H, Morse HC, III (2009) IRF8 regulates myeloid and B lymphoid lineage diversification. *Immunol Res* 43:109–117.
38. Holtschke T, et al. (1996) Immunodeficiency and chronic myelogenous leukemia-like syndrome in mice with a targeted mutation of the ICSBP gene. *Cell* 87:307–317.
39. Wu CY, Maeda H, Contursi C, Ozato K, Seder RA (1999) Differential requirement of IFN consensus sequence binding protein for the production of IL-12 and induction of Th1-type cells in response to IFN-gamma. *J Immunol* 162:807–812.
40. Hobeika E, et al. (2006) Testing gene function early in the B cell lineage in mb1-cre mice. *Proc Natl Acad Sci USA* 103:13789–13794.
41. Hardy RR, Carmack CE, Shinton SA, Kemp JD, Hayakawa K (1991) Resolution and characterization of pro-B and pre-pro-B cell stages in normal mouse bone marrow. *J Exp Med* 173:1213–1225.
42. DeKoter RP, et al. (2010) Regulation of follicular B cell differentiation by the related E26 transformation-specific transcription factors PU.1, Spi-B, and Spi-C. *J Immunol* 185:7374–7384.
43. Derudder E, et al. (2009) Development of immunoglobulin lambda-chain-positive B cells, but not editing of immunoglobulin kappa-chain, depends on NF-kappaB signals. *Nat Immunol* 10:647–654.
44. Guinamard R, Okigaki M, Schlessinger J, Ravetch JV (2000) Absence of marginal zone B cells in Pyk-2-deficient mice defines their role in the humoral response. *Nat Immunol* 1:31–36.
45. Martin F, Oliver AM, Kearney JF (2001) Marginal zone and B1 B cells unite in the early response against T-independent blood-borne particulate antigens. *Immunity* 14: 617–629.
46. Lee CH, et al. (2006) Regulation of the germinal center gene program by interferon (IFN) regulatory factor 8/IFN consensus sequence-binding protein. *J Exp Med* 203: 63–72, and errata (2006) 203:475 and (2008) 205:1507.
47. Kubagawa H, et al. (2015) Nomenclature of Toso, Fas apoptosis inhibitory molecule 3, and IgM FcR. *J Immunol* 194:4055–4057.
48. Wang H, Coligan JE, Morse HC, III (2016) Emerging functions of natural IgM and its Fc receptor FCMR in immune homeostasis. *Front Immunol* 7:99.
49. Smulski CR, Eibel H (2018) BAFF and BAFF-receptor in B cell selection and survival. *Front Immunol* 9:2285.
50. Hatok J, Racay P (2016) Bcl-2 family proteins: Master regulators of cell survival. *Biomol Concepts* 7:259–270.
51. Sochalska M, et al. (2016) Conditional knockdown of BCL2A1 reveals rate-limiting roles in BCR-dependent B-cell survival. *Cell Death Differ* 23:628–639.
52. Tamura T, Thotakura P, Tanaka TS, Ko MS, Ozato K (2005) Identification of target genes and a unique *cis* element regulated by IRF-8 in developing macrophages. *Blood* 106:1938–1947.
53. Kurotaki D, et al. (2018) Transcription factor IRF8 governs enhancer landscape dynamics in mononuclear phagocyte progenitors. *Cell Rep* 22:2628–2641.
54. Basso K, Dalla-Favera R (2012) Roles of BCL6 in normal and transformed germinal center B cells. *Immunol Rev* 247:172–183.
55. Klein U, et al. (2003) Transcriptional analysis of the B cell germinal center reaction. *Proc Natl Acad Sci USA* 100:2639–2644.
56. Cattoretti G, et al. (2006) Stages of germinal center transit are defined by B cell transcription factor coexpression and relative abundance. *J Immunol* 177:6930–6939.
57. Rickert RC, Roes J, Rajewsky K (1997) B lymphocyte-specific, Cre-mediated mutagenesis in mice. *Nucleic Acids Res* 25:1317–1318.
58. Aliberti J, et al. (2003) Essential role for ICSBP in the in vivo development of murine CD8alpha+ dendritic cells. *Blood* 101:305–310.
59. Tsujimura H, Tamura T, Ozato K (2003) Cutting edge: IFN consensus sequence binding protein/IFN regulatory factor 8 drives the development of type I IFN-producing plasmacytoid dendritic cells. *J Immunol* 170:1131–1135.
60. Muto A, et al. (2004) The transcriptional programme of antibody class switching involves the repressor Bach2. *Nature* 429:566–571.
61. Krzyzak L, et al. (2016) CD83 modulates B cell activation and germinal center responses. *J Immunol* 196:3581–3594.
62. De Silva NS, Klein U (2015) Dynamics of B cells in germinal centres. *Nat Rev Immunol* 15:137–148.
63. Dent AL, Shaffer AL, Yu X, Allman D, Staudt LM (1997) Control of inflammation, cytokine expression, and germinal center formation by BCL-6. *Science* 276:589–592.
64. Fukuda T, et al. (1997) Disruption of the Bcl6 gene results in an impaired germinal center formation. *J Exp Med* 186:439–448.
65. Ye BH, et al. (1997) The BCL-6 proto-oncogene controls germinal-centre formation and Th2-type inflammation. *Nat Genet* 16:161–170.
66. Johnston RJ, et al. (2009) Bcl6 and Blimp-1 are reciprocal and antagonistic regulators of T follicular helper cell differentiation. *Science* 325:1006–1010.
67. Tunyaplin C, et al. (2004) Direct repression of prdm1 by Bcl-6 inhibits plasmacytic differentiation. *J Immunol* 173:1158–1165.
68. Saito M, et al. (2007) A signaling pathway mediating downregulation of BCL6 in germinal center B cells is blocked by BCL6 gene alterations in B cell lymphoma. *Cancer Cell* 12:280–292.
69. Shaffer AL, et al. (2002) Blimp-1 orchestrates plasma cell differentiation by extinguishing the mature B cell gene expression program. *Immunity* 17:51–62.
70. Ochiai K, et al. (2013) Transcriptional regulation of germinal center B and plasma cell fates by dynamical control of IRF4. *Immunity* 38:918–929.
71. Wang H, Ye J, Arnold LW, McCray SK, Clarke SH (2001) A VH12 transgenic mouse exhibits defects in pre-B cell development and is unable to make IgM+ B cells. *J Immunol* 167:1254–1262.
72. Ring AM, et al. (2012) Mechanistic and structural insight into the functional dichotomy between IL-2 and IL-15. *Nat Immunol* 13:1187–1195.
73. Yan M, et al. (2016) Cutting edge: Expression of IRF8 in gastric epithelial cells confers protective innate immunity against *Helicobacter pylori* infection. *J Immunol* 196: 1999–2003.
74. Cinamon G, Zachariah MA, Lam OM, Foss FW, Jr, Cyster JG (2008) Follicular shuttling of marginal zone B cells facilitates antigen transport. *Nat Immunol* 9:54–62.
75. Jain S, et al. (2015) IL-21-driven neoplasms in SJL mice mimic some key features of human angioimmunoblastic T-cell lymphoma. *Am J Pathol* 185:3102–3114.